Universal Journal of Green Chemistry
https://ojs.wiserpub.com/index.php/UJGC/

Research Article

Optimization of Batch Adsorption Study Parameters of Acid Dyes onto Spent Brewery Grains

Rukkesh J, Gomathi Priya P*

Department of Chemical Engineering, Alagappa College of Technology, Anna University, Chennai 600025, Tamil Nadu, India
E-mail: pgpriyachem@gmail.com

Received: 3 January 2024; **Revised:** 19 March 2024; **Accepted:** 9 July 2024

Abstract: The exploration of economical and nature friendly adsorbents for dye elimination from effluent is a promising area of research, driven by the need for sustainable and economically viable solutions. This work deals with the adsorption features of Acid Blue 25 (AB25) and Acid Green 25 (AG25) dyes from aqueous solutions using spent brewery grains (SBG). After brewing process, the obtained residue consists of spent grains. Optimum conditions for AB25 & AG25 removal were found to be at pH 2, adsorbent dosage as 0.8 and 1 g/L of solution respectively and equilibrium time was found to be 60 mins. In order to adjudicate the adsorption process, analysis was carried out with kinetic and isothermal two parameter and three parameter models. The results were discovered to fit most with the pseudo-second-order (R^2 = 0.990) for the kinetics and the Langmuir isotherm (R^2 = 0.993) for the adsorption isotherms. The isotherms and kinetics verified that SBG had a high value of adsorption capacity. Experiment results pointed out SBG is one of the best adsorbent that eco-friendly, economical, readily accessible, and efficient on the removal of AB25 and AG25 dyes from aqueous solution.

Keywords: adsorption, spent brewery grains (SBG), acid blue 25 (AB25), acid green 25 (AG25), adsorption isotherms, kinetic models

1. Introduction

Dyes are used as colouring agent in many industries including textile, leather, cosmetics, paper, printing, plastic, pharmaceuticals, and food[1]. It is predictable that more than 100,000 commercially available dyes with over 7 × 10^5 tonnes of dye stuff produced annually[2]. Residual dyes are the major contributors to colour in wastewaters generated from textile and dye manufacturing industries, etc.,[3]. Each dye is unique and can cause harmful effects to environment and to living organisms when untreated. As well as 10,000 dyestuffs were produced annually and above 700,000 metric tons of dyes are available globally in terms of commerce[4]. The release of untreated coloured effluent into the water bodies causes environmental issues such as oxygen content reduction in water and decreased sunlight penetration, which put the life of aquatic animals and plants in peril. Moreover, the industrial wastewater containing dyes is mostly connected with poisonous and carcinogenic effect to the human beings[5,6]. Many methods been followed for dye removal but a new novel material is always needed as the already existing methods are expensive. Dyes are among the pollutants that have stringent restrictions on disposal[7]. In order to meet the current regulations, industries have to utilize technologies to reduce pollution prior to discharge. They are typically categorized as physical, chemical and biological treatment[8]. Now, the major environmental concern is to remove these dyes before entering into water stream. Various techniques like

DOI: https://doi.org/10.37256/ujgc.2220244204

adsorption[9], oxidation[10], biological treatment[11], coagulation[12], electrochemical and radiation[13] biosorption has been used to remove dyes from industrial effluent since long time[14], among these techniques, the adsorption is considered an effective and economical technique as well as relatively superior to other techniques because of inexpensive, simplicity of design, availability and ability to treat dyes in a more concentrated form[15–17]. The dye is adsorbed using a variety of adsorbed materials: peat[18], silica[19], chitin[20] and agriculture waste as adsorbent[21]. This adsorbent material exhibited variable (low) adsorption capacity therefore, it is necessary to develop new adsorbents having high adsorption capacity and should be cheap and easily available in market[22].

The alternatives considered in dye removal using adsorption included both synthetic and natural materials; Nevertheless, the usage of natural resources has increased quickly. In addition to being environmentally friendly, naturally occurring materials and wastes enhance the gathering of inexpensive adsorbents[22]. It is greatly desired that activated carbon be used in the adsorption process. Because of its huge specific surface area and high cost of manufacture and regeneration, activated carbon has a high adsorption capacity. However, the procedure is still quite expensive, making it impractical in many underdeveloped nations[23,24].

Spent brewery grains (SBG) is one of the residues obtained from brewing industry. The grains which are processed in the brewing process and mainly used as cattle feed also in food industry. SBG can be employed as an alternative material like activated carbon used to removes colour and other soluble organic pollutants from textile effluent. Dissolved organics are adsorbed on spent brewery grains surface which used as adsorbent material for treating textile dye waste water. The adsorbent material is one of the best green approaches to handle textile dye waste water which may reduce the environmental toxicity. This study shows that SBG can be used as a viable option as it is cheap and readily available. The quantity of usage of spent grains are very less, thus using SBG can also reduce wastage to the environment.

The primary focus of this paper is the impact of the initial dye concentration, pH, adsorbent dosage and contact time for adsorption by batch method as they greatly impact the adsorption capacity of the SBG. In this study, the dyes degradation using adsorbent as SBG to optimize the parameters for kinetic studies and isotherm studies in two and three parameter models.

2. Materials and methods

2.1 *Material preparation*

The local brewing company in Chennai was the source of the spent brewery grains. The obtained grains were dried overnight, washed with distilled water then air dried for 12 h. It was soaked in a solution of 1 M H_2SO_4 drained and again washed with distilled water and dried in a hot air oven for 24 h at 60 °C. The material was ground and sieve separated to achieve uniform size of 300 μm. No impurities were found in the material after grinding and meshing. Analytical grade AB25 dye having molecular weight of 416.4 g/mol and AG25, molecular weight of 622.6 g/mol was acquired via Sigma Aldrich and utilized without additional purification also the characteristics of textile dyes were shown in the Table 1. High purity laboratory grade reagents were used for the experiments.

Table 1. Characteristics of textile dyes

Characteristics	AB25 DYE	AG25 DYE
Molecular Formula	$C_{20}H_{13}N_2NaO_5S$	$C_{28}H_{23}N_2NaO_8S_2$
Structure	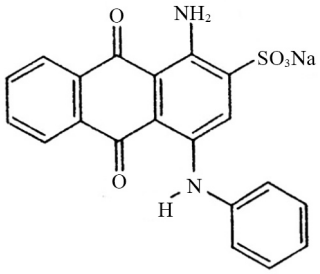	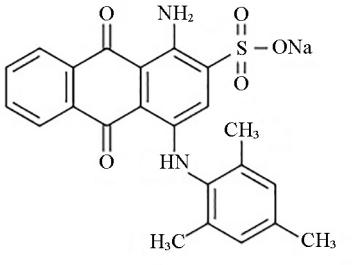
Molecular Weight	416.4 g/mol	622.6 g/mol

2.2 *Design of batch experiments*

The batch experiments were conducted using AB25 and AG25 dyes of aqueous solution utilizing SBG as adsorbent. All experiments were done with 30 mL incubations in a 100 mL Erlenmeyer flask. The aqueous dyes were incubated with SBG on orbital shaker (Scigenics Biotech PVT ltd) at 150 rpm. The absorbance was calculated using UV spectrophotometer UV-1800 Shimadzu Corp, at predetermined wavelengths for the respective dyes for AB25 at a wavelength of 600 nm and for AG25 a wavelength of 642 nm is selected. The effects of contact time, initial concentration, pH, and adsorbent dosage were investigated with the following range of parameters in 150 rpm. The contact time (0–100 min) with 5 min intervals were varied. For the effect of initial dye concentration, the aqueous dye solution concentrations were varied from 30–150 mg/L. Both dyes pH values ranged from 2 to 8. The dosage of the adsorbent (2–10 g) was adjusted. An orbital shaker was used to shake the flasks at 150 rpm. The contact time was studied at regular time interval. Dye solutions with a pH ranging from 1–8 were prepared by adjusting the desired value using either 0.1 M NaOH or 0.1 M HCl solution according to the need. 0.2–1 g of the adsorbent dosage was agitated at 150 rpm at varying time intervals and then absorbance was measured. After samples were taken out at the proper intervals, they were centrifuged at 4000 rpm, and the absorbance for the experiments was recorded. All the experiments were conducted for three times to get better accuracy in room temperature at 25 °C.

2.3 *Adsorption studies*

Using the following equations, the dye removal percentage and amount adsorbed were determined. Equations (1) and (2)

$$Dye\ removal\ (\%) = \frac{(C_0 - C_t)\,100}{C_0} \tag{1}$$

$$q_e = \frac{(C_0 - C_e)\,V}{M} \tag{2}$$

where C_0 and C_t (mg/L) are the liquid-phase concentrations of dye at initial and at any time, respectively. q_e (mg/g) is the equilibrium adsorption amount, V (L) is the volume of the solution and M (g) is the mass of dry sorbent used. C_e (mg/L) concentration at equilibrium.

3. Adsorption theoretical background

3.1 *Adsorption isotherms*

Both two- and three-parameter models were fitted to the batch equilibrium data, and linear regression was used to determine the parameters. The models examined were Langmuir, Freundlich, Harkins Jura, Temkin, Hill, Redlich Peterson, Jovanovich multilayer, Toth models. The results obtained from the initial dye concentration experiment were used for the adsorption isotherm studies.

3.1.1 *Langmuir isotherm*

Though it was initially developed to explain gas-solid phase adsorption, Langmuir adsorption is also used to compare and measure the adsorptive capacity of different adsorbents[25]. Langmuir isotherm accounts for the surface coverage by balancing the relative rates of adsorption and desorption (dynamic equilibrium). Adsorption is proportional to the fraction of the surface of the adsorbent that is open while desorption is proportional to the fraction of the adsorbent surface that is covered[26]. This model is based on monolayer adsorption of dye ions on the surface of SBG active sites and is expressed in linear form as shown in Equation (3)[26]:

$$\frac{C_e}{Q_e} = \frac{1}{Q_{max}\, K_l} + \frac{C_e}{Q_{max}} \tag{3}$$

where C_e is concentration of adsorbate at equilibrium (mg/g), K_l is Langmuir constant related to adsorption capacity (mg/g). Q_{max} (mg/g) is the maximum adsorption uptake. Q_e (mg/g) is adsorption uptake at equilibrium.

3.1.2 *Freundlich isotherm*

The Freundlich isotherm can be used to describe adsorption processes on surfaces that are heterogonous[27]. An expression defining the surface heterogeneity and the exponential distribution of active sites and their energies may be found in this isotherm[28]. The linear form of the Freundlich isotherm is shown in Equation (4)[29]:

$$\log Q_e = \log k_f + \frac{1}{n} log C_e \tag{4}$$

where k_f is Freundlich constant (mg/g) and n is intensity of adsorption (dimensionless).

3.1.3 *Harkin-jura isotherm*

Adsorbents with heterogeneous pore distribution may experience multilayer adsorption on their surface, according to the Harkin-Jura isotherm model[30]. Equation (5) displays the equation in its linear form[31].

$$\frac{1}{{Q_e}^2} = \frac{B}{A} - \left(\frac{1}{A}\right) \log C_e \tag{5}$$

where the Harkin-Jura constants B and A can be found by graphing $1/{Q_e}^2$ against $\log C_e$.

3.1.4 *Temkin isotherm*

The Temkin isotherm model assumes that as surface coverage increases, the heat of adsorption of all molecules in the layer drops linearly, accounting for the impact of indirect adsorbate/adsorbate interactions on the adsorption process[32]. Only an intermediate range of ion concentrations can be used with the Temkin isotherm[33]. The linear form is shown in Equation (6)[34]:

$$Q_e = \frac{R_t}{b} \ln k_t + \frac{R_T}{b} \ln C_e \tag{6}$$

where k_t is the Temkin isotherm constant (L/g) and b is the Temkin constant, which is correlated with the heat of sorption (J/mol).

3.1.5 *Hill isotherm*

The Hill isotherm equation describes the binding of different species onto homogeneous substrates. As per this model, adsorption is thought to be a cooperative process in which different binding sites on the same adsorbent are affected by adsorbates at one site[35]. This isotherm's linear form is expressed as given in Equation (7)[36]:

$$\log \frac{Q_e}{Q_H - Q_e} = n_H \log C_e - \log K_d \tag{7}$$

where K_d and n_H are the Hill constants, Q_H is the maximum adsorption capacity (mg/g).

3.1.6 *Redlich-peterson isotherm*

Three parameters are included in this empirical isotherm model. Since it incorporates components from the Freundlich and Langmuir equations, the adsorption mechanism is mixed and does not adhere to the ideal of monolayer adsorption[37]. The model equation is given in Equation (8)[38]:

$$Q_e = \frac{AC_e}{1 + BC_e^{\beta}} \tag{8}$$

where A is Redlich-Peterson isotherm constant (L/g), B is constant (L/mg), β is exponent that lies between 0 and 1, C_e is equilibrium liquid-phase concentration of the adsorbent (mg/L), and Q_e is equilibrium adsorbate loading on the adsorbent (mg/g).

3.1.7 *Jovanovic isotherm*

In addition to the Langmuir model's underlying assumptions, the Jovanovic model also considers the potential for certain mechanical interactions between the adsorbent and adsorbate[39]. The linear form of the Jovanovic isotherm is expressed as shown in Equation (9)[40]:

$$\ln Q_e = \ln Q_{max} - e^{-k_j C_e} e^{k_{k_j} C_e} \tag{9}$$

where Q_{max} is the highest amount of adsorbate absorbed from the plot of ln Q_e versus C_e, k_j, k_{k_j} is the Jovanovic constant, and Q_e is the amount of adsorbate in the adsorbent at equilibrium (mg/g).

3.1.8 *Toth isotherm*

Another empirical adjustment to the Langmuir equation that aims to lower the discrepancy between experimental data and the expected value of equilibrium data is the Toth isotherm[39]. The most beneficial application of this model is in the description of heterogeneous adsorption systems that meet both the low- and high-end adsorbate concentration boundaries. Equation (10) is a linear form that can be obtained by rearranging the Toth isotherm[41]:

$$\ln (Q_e^n / (Q_m^n - Q_e^n)) = n \ln K_L + n \ln C_e \tag{10}$$

where K_L is Toth isotherm constant (mg/g) and n is surface heterogeneity parameter. Q_m is maximum uptake of adsorbate obtained.

3.2 *Adsorption kinetic studies*

Adsorption kinetic models play a crucial role in the design of the adsorption system, not only in terms of adsorption capacity but also in the rate estimation of the removal process. Moreover, kinetic methods describe the mechanism of substance transfer and determines the rate limiting step, and that is based on the physio-chemical property of the adsorbent and mass transport process[42]. Understanding the dynamics of the adsorption process in terms of the order of rate constant required processing of the kinetic adsorption data.

3.2.1 *Pseudo-first-order kinetic model*

According to this model, the amount of solid absorption over time and the difference in saturation concentration determine how quickly solute uptake changes over time. The kinetics of the adsorption process typically follow the pseudo-first-order rate found in Equation (11), with diffusion across a boundary coming before the reaction[43]:

$$\log(q_e - q_t) = \log q_e - \frac{k_1}{2.303}t \tag{11}$$

The pseudo-first order kinetic model rate constant is represented by k_1 (L/min).

3.2.2 *Pseudo-second-order model*

The pseudo-second-order kinetic model was first put forth by Blanchard et al. in 1980[44]. In the later years, Ho and MacKay[45] modified this model and applied for the removal of pollutant using different adsorbents, which is widely in use by many researchers in the adsorption studies of wastewater pollutants removal. The pseudo-second-order model describes the adsorption process, in which chemisorption acts as the rate-control.

A pseudo-second-order model could be used to describe the sorption kinetics as Equation (12)[45];

$$\frac{t}{q_t} = \frac{1}{k_2 q_e^2} + \frac{t}{q_e} \tag{12}$$

where the amount of the adsorbate that the adsorbent absorbs at time t and equilibrium is denoted by q_t (mg/g) and q_e (mg/g), respectively. The pseudo second order rate constant is represented as k_2 (g/mg min).

3.2.3 *Elovich model*

The Elovich model is a widely used kinetic model that describes the adsorption of adsorbates onto heterogeneous surfaces. This model is particularly useful for describing chemisorption processes, which involve chemical bonding between the adsorbate and the adsorbent. The heterogeneous adsorption sites of the adsorbent are assumed to exhibit varying activation energies during the removal process by the Elovich model. Equation (13) provides the Elovich kinetic model in the following manner[46].

$$q_t = \frac{1}{\beta}\ln(\alpha\beta) + \frac{1}{\beta}\ln t \tag{13}$$

where α (mg/g·min) is the initial rate of adsorption and β (g/mg) is the Elovich model constant.

3.2.4 *Intra-particle diffusion model*

The intra-particle diffusion model developed by Weber and Morris provides valuable insights into the adsorption kinetics and mechanisms, particularly highlighting the role of internal diffusion within the adsorbent's porous structure. Equation (14) illustrates the homogeneous porous structure of the adsorbent and intra-particle diffusion as the rate-limiting step of an adsorption system. The assumption of intraparticle diffusion is based on the transport of the adsorbate through the internal porous structure of the adsorbent and diffusion in the solid[47]:

$$q_t = k_{wm}\, t^{0.5} + I \tag{14}$$

where k_{wm} denotes the constant of intra-particle diffusion model (mg/g $min^{0.5}$) and I indicate the boundary layer thickness (mg/g).

4. Result and discussion

4.1 *The effect of contact time, initial dye concentration, pH and adsorbent dosage*

The effect of contact time using AB25 and AG25 by SBG 100 mg/L for biosorbent dosage 0.5 g was studied. It was noted that for AB25 and AG25 dyes, the highest removal was discovered to happen at 45 and 60 mins respectively. As seen in (Figure 1), this suggests that the equilibrium removal efficiency increases with increasing dye-adsorbent contact duration. The reason behind this is that with longer interaction with the dye molecules higher the adsorption of the dye molecules to the SBG, this may be due to electrostatic attraction force between SBG and aqueous dyes[48]. As the time passes the number of active sites in the SBG decreases thus the removal percentage also decreases.

Initial dye concentration acts as a key motivator to get beyond all of the dye's mass transfer resistances between the aqueous and solid phases, increasing the dye's adsorption. Because of a favourable solute to biosorbent site ratio, the influence of dye concentration on biosorption efficiency is characterized by higher removal percentages at lower concentrations. At higher concentrations, adsorption sites become saturated, leading to a decrease in removal efficiency. Understanding these dynamics is essential for optimizing biosorption processes, ensuring effective dye removal, and designing efficient wastewater treatment systems. By identifying optimal concentration ranges and adjusting biosorbent dosages accordingly, it is possible to achieve high adsorption efficiencies even in varying operational conditions. At 100 mg/L the removal percentage is higher for both dyes shown in (Figure 1). The number of active sites present in the SBG is a primary factor for the removal percentage of the dye. The study of the effect of pH on dye adsorption is essential for optimizing the removal process. pH influences the adsorption capacity through changes in surface charge interactions, the ionization of functional groups, and electrostatic forces.

Additionally, pH affects the color and solubility of dye solutions, which can impact both the adsorption process and the analytical methods used to measure dye concentration. Understanding these pH-dependent behaviours is particularly important for anionic dyes, such as acid dyes, and is crucial for designing effective wastewater treatment systems.

The initial pH of the solution plays a crucial role in the biosorption of dyes by influencing the surface charge of the biosorbent. As the pH increases, the surface becomes more negatively charged, which can lead to electrostatic repulsion of anionic dyes, reducing their adsorption efficiency. Understanding and controlling the pH is essential for optimizing the biosorption process and achieving effective dye removal from wastewater. This knowledge helps in designing better treatment systems and selecting the appropriate conditions for different types of dyes and biosorbents. The max removal was found at 2 for both AG25 and AB25 shown in Figure 1.

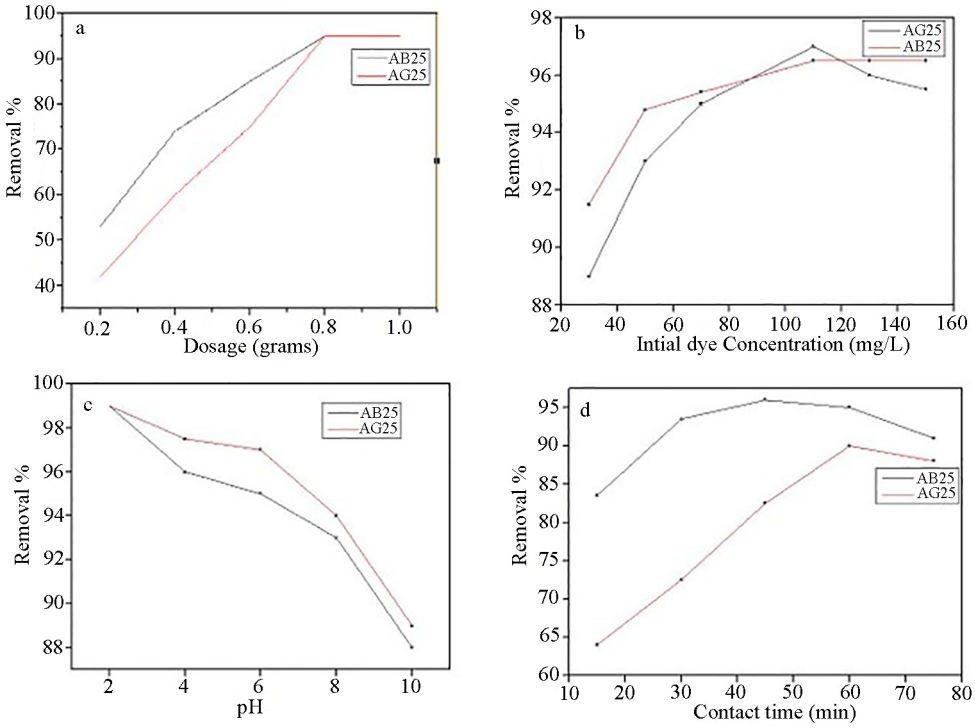

Figure 1. (**a**) Effect of adsorbent dosage on AB25, AG25 (**b**) Effect of initial dye concentration on AB25, AG25, (**c**) Effect of pH on AB25, AG25, (**d**) Effect of contact time on AB25, AG25

The effect of adsorbent dosage was conducted for 0.2 g to 1 g. The increase in the removal of AG25 and AB25 dyes with increasing biosorbent dosage can be attributed to the greater surface area and the availability of more biosorption sites. The eventual plateau in removal capacity is due to the saturation of these sites, limitations in intra-particle diffusion, and potential agglomeration of biosorbent particles. Understanding these dynamics is essential for optimizing biosorption processes and designing efficient wastewater treatment systems. For AB25 and AG25 dye gives high removal percentage for 0.8 g shown in Figure 1. The observed increase in removal capacity with increasing adsorbent dose can indeed be explained by the presence of more adsorption sites with a larger surface area.

4.2 *Adsorption isotherms*

Adsorption isotherms recommend useful specifications for determining the uptake mechanism and adsorbent properties. In this work, the two parameter and three parameter adsorption isotherms were applied to find out the adsorption mechanism. The Langmuir model shows regression value of 0.7473 and 0.9867 for AB25 and AG25 Dye respectively. The K_l value is less than 1 which shows the favorable conditions for the Langmuir isotherm model, Possibility of monolayer adsorption. The Langmuir model fits best for AB25 dye. For Freundlich model the regression value are 0.9013 and 0.8931 for AB25 and AG25 dye respectively. The n value was found to be 1.5 for both dyes, this clearly shows that the condition for Freundlich model is not favorable. The plot for Langmuir and Freundlich model is given in the Figure 2. In Harkin-Jura model isotherm constants are found as A = 0.2762 and B = 0.5865 for AB25 dye which is below unity, Thus, the conditions are considered to be favorable.

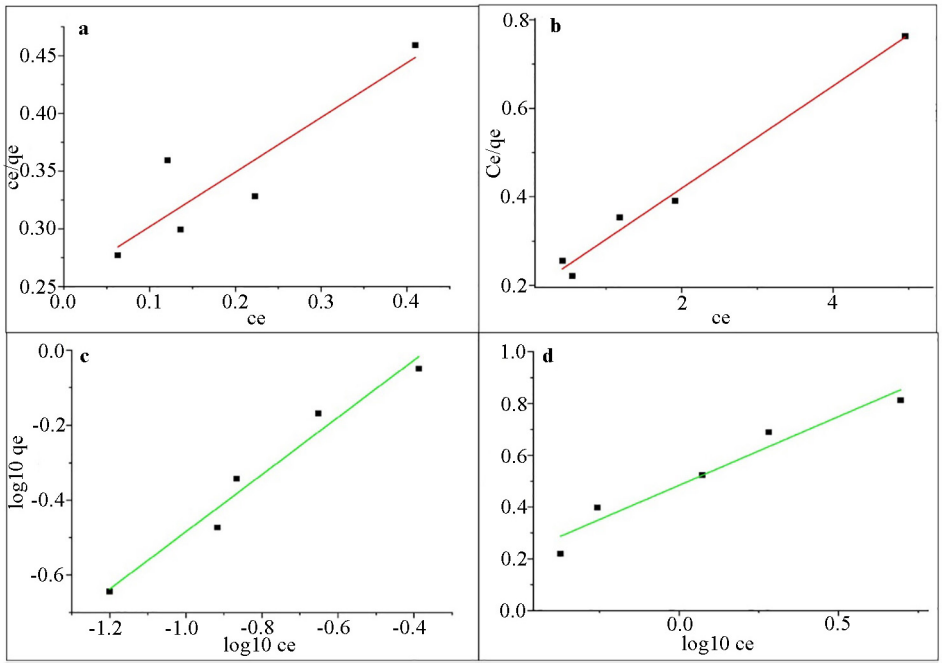

Figure 2. (**a**) Langmuir plot for AB25 dye. (**b**) Langmuir plot for AG25 dye. (**c**) Freundlich plot for AB25 dye. (**d**) Freundlich plot for AG25 dye

The conditions are not suitable for the removal of AG25 dye because $A = 21.155$ and $B = 2.0811$ for AG25 dye are both over unity. The adsorption is better for AB25 than AG25 by Harkins—Jura model. In Temkin Model $B = 24.3693$ and 5.781 (J/mg), higher the value lowers the adsorption rate as the increase in B decreases the adsorption due to lower surface coverage. K_t shows the adsorption uptake. The Harkin-Jura and Temkin model were plotted and the plot is given in the Figure 3. Langmuir, Freundlich, Harkin-Jura and Temkin model are two parameter models. The two parameter models were fitted and studied and the results are tabulated in Table 2.

Table 2. Comparison of model parameters for two parameter models for AB25 and AG25 dye

Two Parameter Models	AB25 DYE	AG25 DYE
Langmuir Model	Q_{max}—9.318 (mg/g) K_l—0.4998 L/mg $R^2 = 0.7473$	Q_{max}—8.659 (mg/g) K_l—0.627 L/mg $R^2 = 0.9867$
Freundlich	k_f—6.1083 mg/g n—1.5 $R^2 = 0.9013$	k_f—3.2013 mg/g n—1.5 $R^2 = 0.8931$
Harkins-Jura	A—0.2762 B—0.5865 $R^2 = 0.8171$	A—21.155 B—2.0811 $R^2 = 0.7058$
Temkin	b—24.3693 (J/mg) k_t—6.393 × 10^4 (L/mg) $R^2 = 0.9622$	b—5.781 (J/mg) k_t—1.649 × 10^3 (L/mg) $R^2 = 0.9719$

In Hill model, Q_H shows the adsorption uptake which is 3.7641 and 6.381 (mg/g) for AB25 and AG25 dye respectively. K_d is the adsorption isotherm constant. n_H value is 1.642 and 1.045 which shows the stability of the adsorbate as it is higher than unity as for Hill model the value under unity shows stability of the model parameter. For R-P model, A and B values are adsorption isotherm constants. β Value shows the favorable condition for R-P model. $\beta = 0.333$ and $\beta = 1.092$ are the values for AB25 and AG25 dye respectively. The Hill and R-P model is fitted and the plot is given in Figure 4.

Jovanovich Multilayer, Q_{max} shows the maximum adsorption uptake, Q_{max} as 15.2 and 5.785 mg/g for AB25 and AG25 dye Respectively. k_j & k_{k_j} values show the favorable condition for J-M model. The regression values are 0.6510 and 0.8800 for the both the dyes.

For Toth Model, regression value is 0.9761 for AB25 dye and 0.9265 for AG25 dye. The Toth model fits the best for AB25 dye. n = 1.5717 and 1.3281 which is above unity this shows the stable condition of the adsorbate. K_l value is above unity this shows the favorable condition for AB25 and AG25 dye. J-M and Toth model is fitted for both the dyes and the plot is given in the Figure 5. Hill, R-P, J-M and Toth models are three parameter model. The three parameter models were studied and the theoretically calculated parameters were tabulated in Table 3.

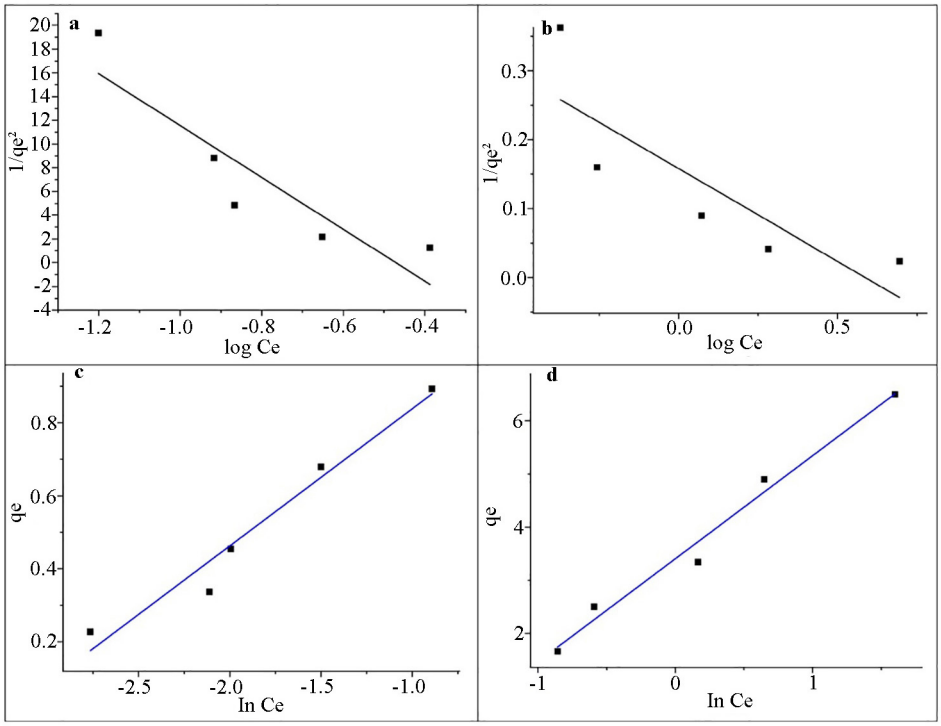

Figure 3. (**a**) Harkins Jura plot for AB25 dye. (**b**) Harkins Jura plot for AG25 dye. (**c**) Temkin plot for AB25 dye. (**d**) Temkin plot for AG25 dye

Table 3. A comparison of the three parameter models for the dyes AG25 and AB25

Three Parameter Models	AB25 DYE	AG25 DYE
Hill	Q_H—3.7641 (mg/g) K_d—0.04962 (L/mg) n_H—1.642 R^2 = 0.9632	Q_H—6.381 (mg/g) K_d—1.5030 (L/mg) n_H—1.045 R^2 = 0.9503
Redlich-Peterson	A—4743.26 (L/mg) B—2772.48 (L/mg) β—0.333 R^2 = 0.7251	A—4953.26 (L/mg) B—480.48 (L/mg) β—1.092 R^2 = 0.9329
Jovanovich Multilayer	Q_{max}—15.2 (mg/g) k_j—0.028 (L/mg) k_{k_j}—1.575 (L/mg) R^2 = 0.6150	Q_{max}—5.785 (mg/g) k_j—0.8250 (L/mg) k_{k_j}—0.02706 (L/mg) R^2 = 0.8800
Toth	Q_m^n—26.659 (mg/g) K_L—10.577 (L/mg) n—1.5717 R^2 = 0.9761	Q_m^n –4.1229 (mg/g) K_L—5.0481 (L/mg) n—1.3281 R^2 = 0.9265

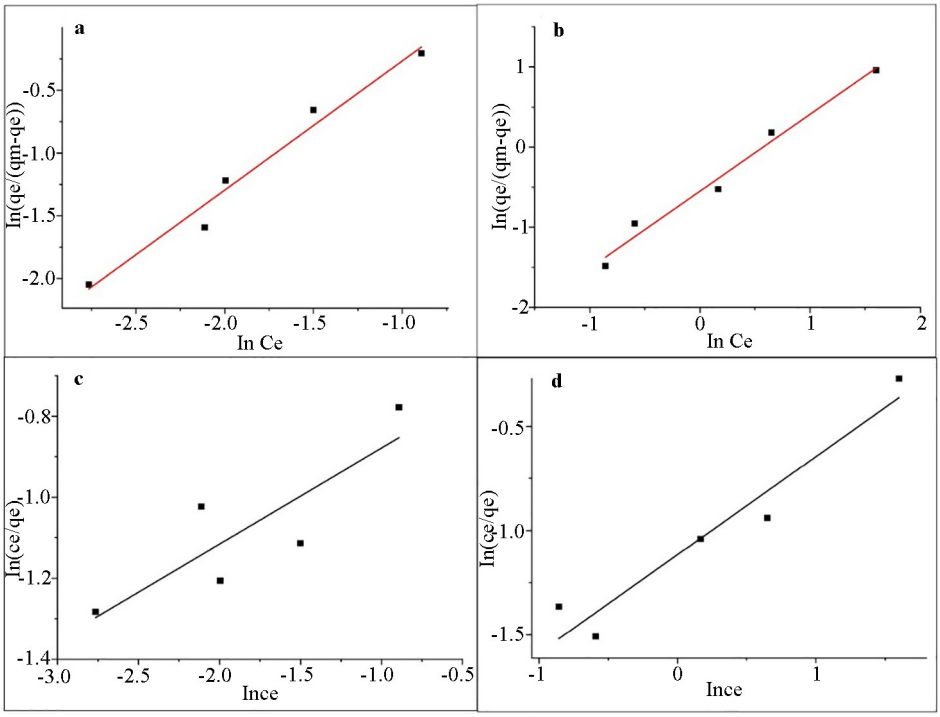

Figure 4. (**a**) Hill isotherm plot for AB25. (**b**) Hill Isotherm plot for AG25. (**c**) Redlich-Peterson plot for AB25. (**d**) Redlich-Peterson plot for AG25

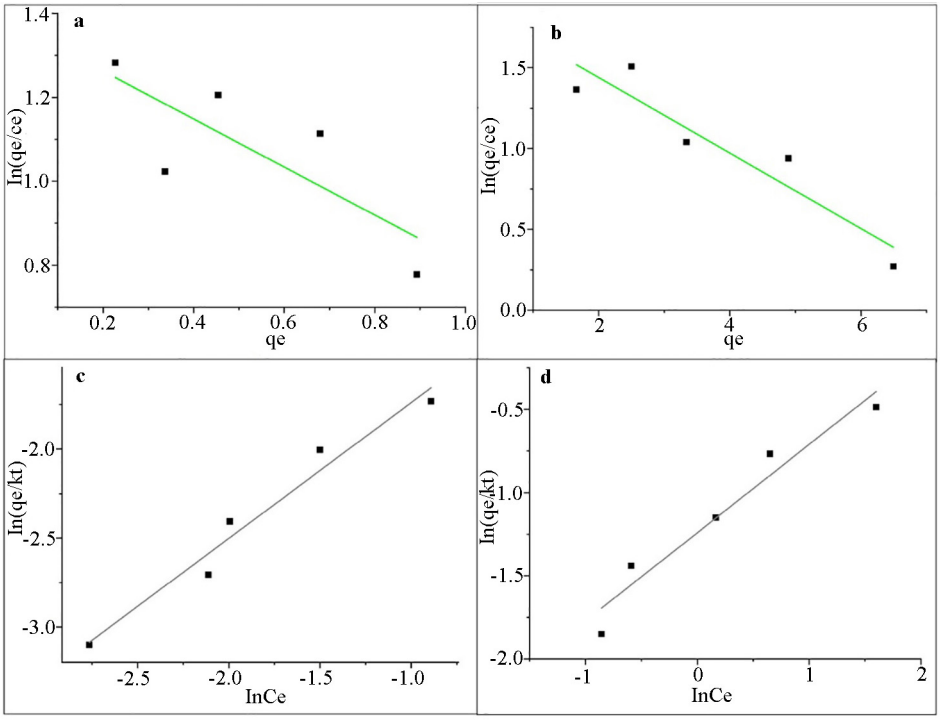

Figure 5. (**a**) Jovanovich Multilayer plot for AB25. (**b**) Jovanovich Multilayer plot for AG25. (**c**) Toth model plot for AB25. (**d**) Toth model plot for AG25

4.3 *Adsorption kinetics*

For the kinetic experiments, Webber Morris, Elovich, and pseudo first and second order were fitted. The lines for the pseudo first order model do not fit the data exactly. The regression value is found to be 0.9219 & 0.9686 for AB25 and AG25 dye respectively. The q_e values are 0.87669 and 6.5487 for AB25 and AG25 dye respectively. For Pseudo second order model the line fits the data points perfectly the regression values are found to be 0.9979 and 0.9819 for AB25 and AG25 dye respectively. Both dyes are fitted using the pseudo second order model. Figure 6 shows the plot for the first and second order kinetic models.

For Elovich model, only some points fit in the model line, the regression value is found to be 0.9230 & 0.9677 for AB25 and AG25 dye respectively. α and β are kinetic model constants. $\beta = 37$ & 0.9915 for AB25 and AG25 dye respectively. As the β is above 1 the conditions are not favorable for AB25 dye. For Intra particle diffusion, AB25 dye data points fits better than AG25 dye. This shows the intra particle adsorption is higher in AB25 than in AG25 dye. The I shows the boundary layer parameter, where it was found to be I = 0.5277 and 2.4489 (mg/g) for AB25 and AG25 dye respectively. As I for AB25 is less than AG25 dye, the intra particle adsorption is more in AG25. Figure 7 displays the curve of the fitted Elovich and Intra particle diffusion models.

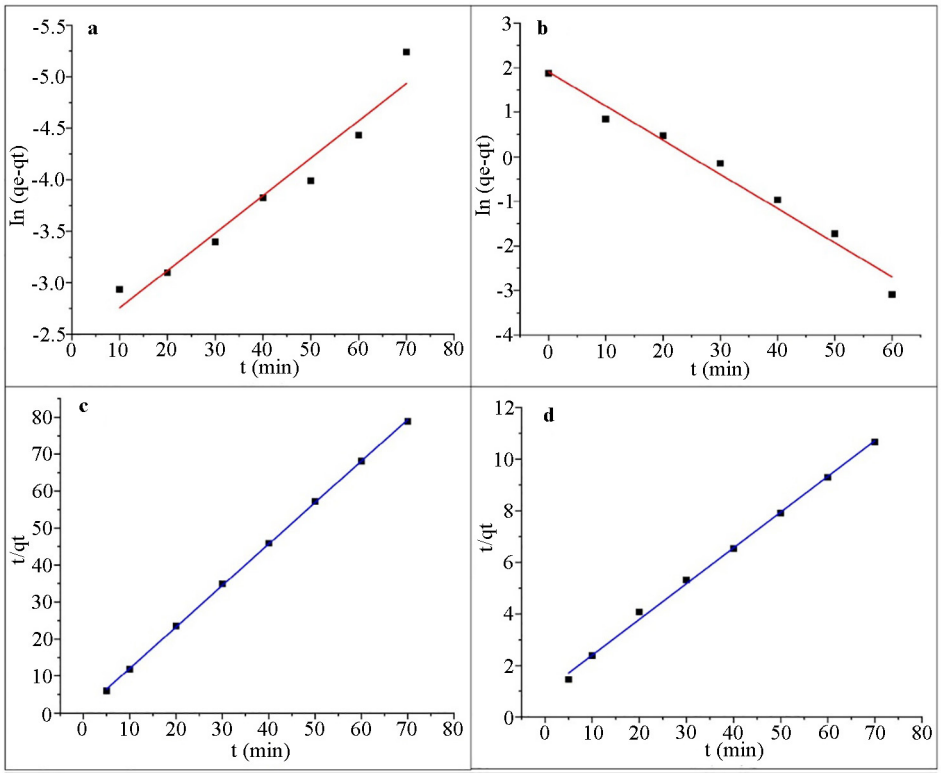

Figure 6. (**a**) Pseudo first order plot for AB25. (**b**) Pseudo first order plot for AG25. (**c**) Pseudo second order plot AB25. (**d**) pseudo second order plot for AG25

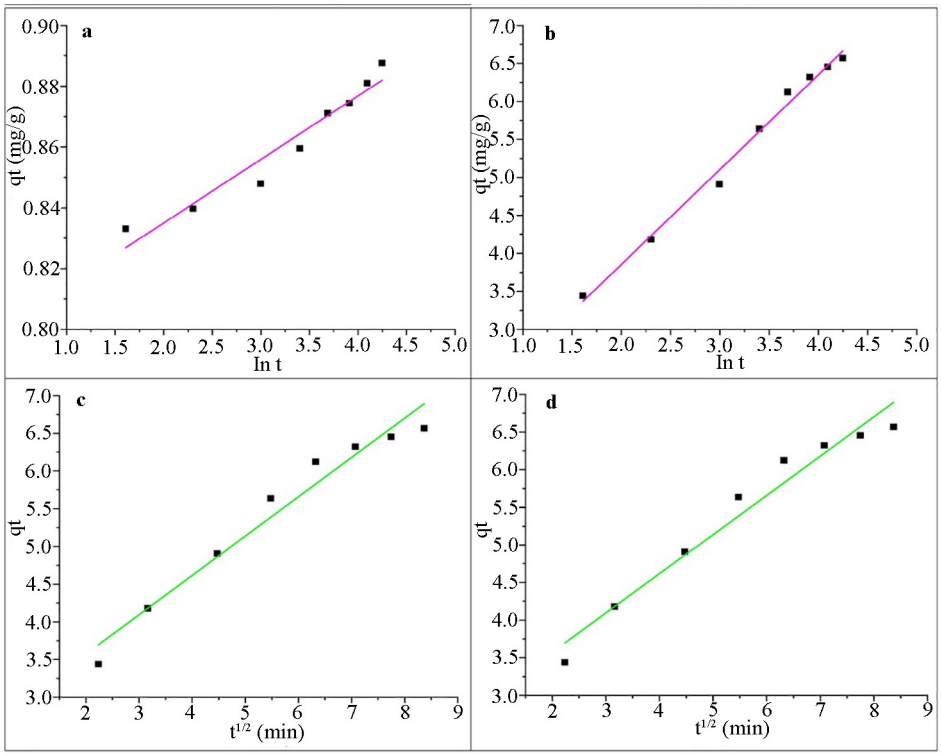

Figure 7. (**a**) Elovich Kinetic plot for AB25. (**b**) Elovich Kinetic plot for AG25. (**c**) Webber-Morris plot for AB25. (**d**) Webber-Morris plot for AG25

The experimental data were used to fit and analyze the kinetic models, and the resultant estimated parameters are listed in Table 4. It was revealed through the isotherm and kinetic investigations that SBG is a practical method for removing dye from aqueous solutions.

Table 4. Kinetic model parameter comparison

Kinetic Models	AB25 DYE	AG25 DYE
Pseudo First order Model	q_e—0.87669 (mg/g) K_1—0.58252 (min^{-1}) R^2 = 0.9219	q_e—6.5487 (mg/g) K_1—0.08540 (min^{-1}) R^2 = 0.9686
Pseudo second order Model	q_e—0.88927 (mg/g) K_2—2.29607 (g/mg · min) R^2 = 0.9979	q_e—7.14911 (mg/g) K_2—0.01889 (g/mg · min) R^2—0.9819
Elovich Model	α—230 (mg/g · min) β—37 (mg/g) R^2 = 0.9230	α—57 (mg/g · min) β—0.9155 (mg/g) R^2 = 0.9677
Webber—Morris Model	k_{wm}—0.0646 (mg/g $min^{0.5}$) I—0.5277 (mg/g) R^2 = 0.9814	k_{wm}—0.4678 (mg/g $min^{0.5}$) I—2.4489 (mg/g) R^2 = 0.8758

5. Conclusions

Low-cost and eco-friendly adsorbents hold significant promise for dye removal from wastewater, offering an alternative that is both sustainable and cost-effective. It was investigated if leftover brewing grains could be used to remove the dyes AG25 and AB25. The experiments were performed as a function of initial dye concentration, dosage, pH, and contact time. The biosorbent capacity was significantly influenced by the pH of the solution, temperature, and initial dye concentration.

Low pH at 2 and high adsorbent dosage like 0.8 g gives high removal percentage for both the dyes. Using AB25 and AG25 dyes, the ideal contact times were determined to be 45 and 60 mins, respectively. This yielded a very intriguing result, with the curve increasing and then decreasing as the time increased. This is because the active sites of SBG fill up over time. Attainment of equilibrium has been analysed using two and three parameter adsorption isotherms. The adsorptive capabilities of SBG for the removal of the dyes AG25 and AB25 were compared using the experimental isotherm constants. The best correlation for dye adsorption was found using the Langmuir isotherm; nevertheless, the Harkins Jura model indicates that AB25 adsorbed more effectively than AG25. In three parameter model, using AG25 dye, the Redlich Peterson adsorption isotherm fits well and Hill and Toth model fits well for both the dyes. According to kinetic studies investigations, pseudo-second order kinetics models were followed by the SBG-based AB25 and AG25 adsorption process. High initial dye concentration gives high removal percentage as the ratio between active sites and the dye molecules is high when compared to low initial concentration. When compared to other materials like fly ash, hardwood sawdust, chitosan, activated carbon, rice husk-based materials, etc., SBG is less expensive and would be a useful and efficient green route for the economically viable treatment of textile dye in waste water. Materials from other studies show good removal percentages for acid dyes, but the materials are not cost-effective.

References

[1] Garg, V. K.; Amita, M.; Kumar, R.; Gupta, R. Basic Dye (Methylene Blue) Removal from Simulated Wastewater by Adsorption Using Indian Rosewood Saw Dust: A Timber Industry Waste. *Dyes Pigments* **2004**, *63*, 243–250.

[2] Lee, J. W.; Choi, S. P.; Thiruvenkatachari, R.; Shim, W. G.; Moon, H. Evaluation of the Performance of Adsorption and Coagulation Processes for the Maximum Removal of Reactive Dyes. *Dyes Pigments* **2006**, *69*, 196–203.

[3] Malik, R.; Ramteke, D. S.; Wate, S. R. Adsorption of Malachite Green on Groundnut Shell Waste Based Powdered Activated Carbon. *Waste Manage.* **2007**, *27*, 1129–1138.

[4] Yagub, M. T.; Sen, T. K.; Ang, H. M. Equilibrium, Kinetics, and Thermodynamics of Methylene Blue Adsorption by Pine Tree Leaves. *Water Air Soil Pollut.* **2012**, *223*, 5267–5282.

[5] Rangabhashiyam, S.; Balasubramanian, P. Adsorption Behaviors of Hazardous Methylene Blue and Hexavalent Chromium on Novel Materials Derived from Pterospermum Acerifolium Shells. *J. Mol. Liq.* **2018**, *254*, 433–445.

[6] Guo, J. Z.; Li, B.; Liu, L.; Lv, K. Removal of Methylene Blue from Aqueous Solutions by Chemically Modified Bamboo. *Chemosphere* **2014**, *111*, 225–231.

[7] Federal Register / Vol. 64, No. 141 / Friday, July 23, 1999 / Proposed Rules. Available online: https://www.govinfo.gov/content/pkg/FR-1999-07-23/pdf/99-17337.pdf (accessed on 2 January 2024)

[8] Gupta, V. K. Application of Low-Cost Adsorbents for Dye Removal—A Review. *J. Environ. Manage.* **2009**, *90*, 2313–2342.

[9] Al-Qodah, Z. Adsorption of Dyes Using Shale Oil Ash. *Water Res.* **2000**, *34*, 4295–4303.

[10] Czerwicka, M.; Stolte, S.; Müller, A.; Siedlecka, E. M.; Gołebiowski, M.; Kumirska, J.; Stepnowski, P. Identification of Ionic Liquid Breakdown Products in an Advanced Oxidation System. *J. Hazard. Mater.* **2009**, *171*, 478–483.

[11] Humphrey, J. L.; Keller, G. E. *Separation Process Technology*; McGraw-Hill: New York, NY, USA, 1997.

[12] Zeng, X.; Ruckenstein, E. Crosslinked Macroporous Chitosan Anion Exchange Membranes for Protein Separations. *J. Membr. Sci.* **1998**, *148*, 195–205.

[13] Xu, B.; Wu, F.; Chen, R.; Cao, G.; Chen, S.; Yang, Y. Mesoporous Activated Carbon Fiber as Electrode Material for High Performance Electrochemical Double Layer Capacitors with Ionic Liquid Electrolyte. *J. Power Sources* **2010**, *195*, 2118–2124.

[14] Crini, G.; Badot, P. M. Application of Chitosan, a Natural Amino Polysaccharide, for Dye Removal from Aqueous Solutions by Adsorption Processes Using Batch Studies: A Review of Recent Literature. *Prog. Polym. Sci.* **2008**, *33*, 399–447.

[15] Al-Ghouti, M. A.; Li, J.; Salamh, Y.; Al-Laqtah, N.; Walker, G.; Ahmad, M. N. M. Adsorption Mechanisms of Removing Heavy Metals and Dyes from Aqueous Solution Using Date Pits Solid Adsorbent. *J. Hazard. Mater.* **2010**, *176*, 510–520.

[16] Wawrzkiewicz, M.; Hubicki, Z. Equilibrium and Kinetic Studies on the Sorption of Acidic Dye by Macroporous Anion Exchanger. *Chem. Eng. J.* **2010**, *157*, 29–34.

[17] Crini, G.; Badot, P. M. Application of Chitosan, a Natural Amino Polysaccharide, for Dye Removal from Aqueous Solutions by Adsorption Processes Using Batch Studies: A Review of Recent Literature. *Prog. Polym. Sci.* **2008**, *33*, 399–447.
[18] Ramakrishna, K. R.; Viraraghavan, T. Dye Removal Using Low-Cost Adsorbents. *Water Sci. Technol.* **1997**, *36*, 189–196.
[19] McKay, G.; Blair, H. S.; Gardner, J. Rate Studies for the Adsorption of Dyestuffs onto Chitin. *J. Colloid Interface Sci.* **1983**, *95*, 108–119.
[20] McKay, G. Analytical Solution Using a Pore Diffusion Model for a Pseudo Irreversible Isotherm for the Adsorption of Basic Dye on Silica. *AIChE J.* **1984**, *30*, 692–697.
[21] Robinson, T.; Chandran, B.; Nigam, P. Removal of Dyes from a Synthetic Textile Dye Effluent by Biosorption on Apple Pomace and Wheat Straw. *Water Res.* **2002**, *36*, 2824–2830.
[22] Ahmad, A. A.; Idris, A.; Mahmoud, D. K. Equilibrium Modelling, Kinetic and Thermodynamic Studies on the Adsorption of Basic Dye by Low-Cost Adsorbent. *J. Adv. Sci. Eng. Res.* **2011**, *1*, 261–277.
[23] Lin, S.; Song, Z.; Che, G.; Ren, A.; Li, P.; Liu, C.; Zhang, J. Adsorption Behaviour of Metal-Organic Frameworks for Methylene Blue from Aqueous Solution. *Microporous Mesoporous Mater.* **2014**, *193*, 27–34.
[24] Duman, O.; Ayranci, E. Adsorptive Removal of Cationic Surfactants from Aqueous Solutions onto High-Area Activated Carbon Cloth Monitored by in Situ UV Spectroscopy. *J. Hazard. Mater.* **2010**, *174*, 359–367.
[25] Elmorsi, T. M. Equilibrium Isotherms and Kinetic Studies of Removal of Methylene Blue Dye by Adsorption onto Miswak Leaves as a Natural Adsorbent. *J. Environ. Prot.* **2011**, *2*, 817–827.
[26] Günay, A.; Arslankaya, E.; Tosun, I. Lead Removal from Aqueous Solution by Natural and Pretreated Clinoptilolite: Adsorption Equilibrium and Kinetics. *J. Hazard. Mater.* **2007**, *146*, 362–371.
[27] Ayawei, N.; Angaye, S. S.; Wankasi, D.; Dikio, E. D. Synthesis, Characterization and Application of Mg/Al Layered Double Hydroxide for the Degradation of Congo Red in Aqueous Solution. *Open J. Phys. Chem.* **2015**, *5*, 56–70.
[28] Ayawei, N.; Ekubo, A. T.; Wankasi, D.; Dikio, E. D. Adsorption of Congo Red by Ni/Al-CO_3: Equilibrium, Thermodynamic and Kinetic Studies. *Orient. J. Chem.* **2015**, *31*, 1307–1318.
[29] Boparai, H. K.; Joseph, M.; O'Carroll, D. M. Kinetics and Thermodynamics of Cadmium Ion Removal by Adsorption onto Nano Zerovalent Iron Particles. *J. Hazard. Mater.* **2011**, *186*, 458–465.
[30] Foo, K. Y.; Hameed, B. H. Insights into the Modeling of Adsorption Isotherm Systems. *Chem. Eng. J.* **2010**, *156*, 2–10.
[31] Okpara, O. G.; Ogbeide, O. M.; Ike, O. C.; Menechukwu, K. C.; Ejike, E. C. Optimum Isotherm by Linear and Nonlinear Regression Methods for Lead (II) Ions Adsorption from Aqueous Solutions Using Synthesized Coconut Shell—Activated Carbon (SCSAC). *Toxin Rev.* **2020**, *40*, 901–914.
[32] Ringot, D.; Lerzy, B.; Chaplain, K.; Bonhoure, J.-P.; Auclair, E.; Larondelle, Y. In Vitro Biosorption of Ochratoxin A on the Yeast Industry By-Products: Comparison of Isotherm Models. *Bioresour. Technol.* **2007**, *98*, 1812–1821.
[33] Shahbeig, H.; Bagheri, N.; Ghorbanian, S. A.; Hallajisani, A.; Poorkarimi, S. A New Adsorption Isotherm Model of Aqueous Solutions on Granular Activated Carbon. *World J. Model. Simul.* **2013**, *9*, 243–254.
[34] Vijayaraghavan, K.; Padmesh, T. V. N.; Palanivelu, K.; Velan, M. Biosorption of Nickel(II) Ions onto Sargassum Wightii: Application of Two-Parameter and Three-Parameter Isotherm Models. *J. Hazard. Mater.* **2006**, *133*, 304–308.
[35] Rania, F.; Yousef, N. S. Equilibrium and Kinetics Studies of Adsorption of Copper(II) on Natural Biosorbent. *Int. J. Chem. Eng. Appl.* **2015**, *6*, 319.
[36] Hamdaoui, O.; Naffrechoux, E. Modelling of Adsorption Isotherms of Phenol and Chlorophenols onto Granular Activated Carbon. Part I. Two-Parameter Models and Equations Allowing Determination of Thermodynamic Parameters. *J. Hazard. Mater.* **2007**, *147*, 381–394.
[37] Brouers, F.; Al-Musawi, T. J. On the Optimal Use of Isotherm Models for the Characterization of Biosorption of Lead onto Algae. *J. Mol. Liq.* **2015**, *212*, 46–51.
[38] Knaebel, S. K. *Adsorbent Selection*; Adsorption Research Inc.: Dublin, OH, USA, 2004.
[39] Jafari Behbahani, T.; Jafari Behbahani, Z. A New Study on Asphaltene Adsorption in Porous Media. *Pet. Coal* **2014**, *56*, 459–466.
[40] Kiseler, A. V. C. Vapour Adsorption in the Formation of Adsorbate Molecule Complexes on the Surface. *Kolloid Zhur* **1958**, *20*, 338–348.
[41] Padder, M. S.; Majunder, C. B. C. Studies on Removal of As (II) and S (V) onto GAC/MnFe. *Compos. Isotherm Studies Error Anal.* **2012**, *23*, 327–372.

[42] Tang, B.; Yao, Y.; Chen, W.; Chen, X.; Zou, F.; Wang, X. Kinetics of Dyeing Natural Protein Fibers with Silver Nanoparticles. *Dyes Pigments* **2018**, *148*, 224–235.
[43] Lagergren, S. About the Theory of So-Called Adsorption of Soluble Substances. *K. Svenska Vetenskapsakad. Handl.* **1898**, *24*, 1–39.
[44] Blanchard, G.; Maunaye, M.; Martin, G. Removal of Heavy Metals from Waters by Means of Natural Zeolites. *Water Res.* **1984**, *18*, 1501–1507.
[45] Ho, Y. S.; McKay, G. Pseudo-Second Order Model for Sorption Processes. *Process Biochem.* **1999**, *34*, 451–465.
[46] Wu, F. C.; Tseng, R. L.; Juang, R. S. Characteristics of Elovich Equation Used for the Analysis of Adsorption Kinetics in Dye-Chitosan Systems. *Chem. Eng. J.* **2009**, *150*, 366–373.
[47] Weber, W. J.; Morris, J. C. Advances in Water Pollution Research: Removal of Biologically Resistant Pollutants from Waste Waters by Adsorption. In *Proceedings of the International Conference on Water Pollution Symposium*; Pergamon Press: Oxford, UK, 1962; pp. 231–266.
[48] Tang, R.; Dai, C.; Li, C.; Liu, W.; Gao, S.; Wang, C. Removal of Methylene Blue from Aqueous Solution Using Agricultural Residue Walnut Shell: Equilibrium, Kinetic, and Thermodynamic Studies. *J. Chem.* **2017**, 8404965. https://doi.org/10.1155/2017/8404965.